HHS Public Access

Author manuscript

Lung Cancer. Author manuscript; available in PMC 2018 October 01.

Published in final edited form as:

Lung Cancer. 2017 October ; 112: 47–56. doi:10.1016/j.lungcan.2017.08.001.

Mig-6 Deficiency Cooperates with Oncogenic Kras to Promote Mouse Lung Tumorigenesis

Jian Liu[1,+], **Sung-Nam Cho**[2,+], **San-Pin Wu**[1], **Nili Jin**[2], **Seyed Javad Moghaddam**[3], **Jennifer L. Gilbert**[5], **Ignacio Wistuba**[4], and **Francesco J. DeMayo**[1,*]

[1]Reproductive & Developmental Biology Laboratory, National Institute of Environmental Health Sciences (NIEHS), Research Triangle Park, NC, USA [2]Department of Molecular and Cellular Biology, Baylor College of Medicine, Houston, TX, USA [3]Department of Pulmonary Medicine, University of Texas MD Anderson Cancer Center, Houston, TX, USA [4]Department of Translational Molecular Pathology, University of Texas, M.D. Anderson Cancer Center, Houston, TX, USA [5]Department of Biology, Maynooth University, Maynooth, Co. Kildare, Ireland

Abstract

Objectives—Lung cancer is the leading cause of cancer related deaths worldwide and mutation activating *KRAS* is one of the most frequent mutations found in lung adenocarcinoma. Identifying regulators of *KRAS* may aid in the development of therapies to treat this disease. The mitogen-induced gene 6 MIG-6 is a small adaptor protein modulating signaling in cells to regulate the growth and differentiation in multiple tissues. Here, we investigated the role of *Mig-6* in regulating adenocarcinoma progression in the lungs of genetically engineered mice with activation of *Kras*.

Materials and Methods—Using the $CCSP^{Cre}$ mouse to specifically activate expression of the oncogenic $Kras^{G12D}$ in Club cells, we investigated the expression of *Mig-6* in $CCSP^{Cre}Kras^{G12D}$-induced lung tumors. To determine the role of *Mig-6* in $Kras^{G12D}$-induced lung tumorigenesis, *Mig-6* was conditionally ablated in the Club cells by breeding $Mig6^{f/f}$ mice to $CCSP^{Cre}Kras^{G12D}$ mice, yielding $CCSP^{Cre}Mig\text{-}6^{d/d}Kras^{G12D}$ mice ($Mig\text{-}6^{d/d}Kras^{G12D}$).

Results—We found that *Mig-6* expression is decreased in $CCSP^{Cre}Kras^{G12D}$-induced lung tumors. Ablation of *Mig-6* in the $Kras^{G12D}$ background led to enhanced tumorigenesis and reduced life expectancy. During tumor progression, there was increased airway hyperplasia, a heightened inflammatory response, reduced apoptosis in $Kras^{G12D}$ mouse lungs, and an increase

*To whom correspondence should be addressed: Francesco J. DeMayo, Ph.D., Senior Principal Investigator, Deputy Chief of the NIEHS Reproductive and Developmental Biology Laboratory (RDBL), and Principle Investigator, Pregnancy and Reproduction Group. Phone: (919) 541-0280, francesco.demayo@nih.gov.
+These authors contributed equally to this work

Author contributions statement

J.L., S.-N.C. and F.J.D. designed the experiments. J.L. and S.-N.C. performed the experiments and data analysis. J.L., S.-N.C., S.-P.W. and F.J.D. wrote the manuscript. N.-l.J. helped analyze the mouse phenotypes. S.J.M., J.L.G. and I.W. characterized mouse lung tumor types and helped Laser Capture Microdissection. F.J.D. supervised the project.

Conflict of interest: The authors have no conflict of interest.

of total and phosphorylated ERBB4 protein levels. Mechanistically, *Mig-6* deficiency attenuates the cell apoptosis of lung tumor expressing $KRAS^{G12D}$ partially through activating the ErbB4 pathway.

Conclusions—In summary, *Mig-6* deficiency promotes the development of $Kras^{G12D}$-induced lung adenoma through reducing the cell apoptosis in $Kras^{G12D}$ mouse lungs partially by activating the ErbB4 pathway.

Keywords

Mig-6 (ERRFI1); *Kras*; ErbB4; Lung cancer/tumor; ErbB signaling; Apoptosis

Introduction

Lung cancer is the leading cause of cancer-related deaths worldwide [1, 2]. Human lung cancers are categorized as non-small cell lung carcinoma (NSCLC) and small cell carcinoma (SCLC) [3, 4]. NSCLC accounts for about 80% of lung cancers and its adenocarcinoma (AD) subtype is found in 30–40% of all lung cancers [5–7]. Genomic analyses have identified somatic mutations in key signaling pathways in lung adenocarcinoma [8]. Activating *Kras* mutations, among the most frequently identified in human tumors, are found in 25–50% of human lung ADs and associated with poor prognosis [9, 10]. Activated *Kras* constitutively turns on *PI3K/AKT* and *RAF/MEK/ERK* signaling pathways, resulting in abnormal cell proliferation and apoptosis [11–15]. *Kras* mutants change the tumor growth microenvironment through the activation of tissue remodeling, inflammation, and angiogenesis [13, 15, 16]. For example, mice with the constitutively active $Kras^{G12D}$ mutant allele develop adenocarcinoma [17]. Identification of modifiers of *Kras* may present targets for treatment of patients with *Kras*-driven AD and one potential regulator of *KRAS* is MIG-6. Downregulation of *MIG-6* has been demonstrated to enhance resistance of *KRAS* mutant human colorectal and gastric adenocarcinoma cells to MEK inhibitors [18], suggesting that *MIG-6* inactivation regulates the properties of cancers having the *KRAS* mutation.

MIG-6, also known as ErbB receptor feedback inhibitor 1 (Errfil) [19], is a ubiquitously expressed scaffold protein that is induced by growth factors or other stress stimuli [20]. MIG-6 modulates growth factor activation by regulating signaling pathways through the alterations of auto-phosphorylations of protein kinases [19, 20]. Downregulated *MIG-6* expression is observed in multiple human cancers, including lung cancer [21–25]. Germline ablation of *Mig-6* in mice results in partial neonatal mortality due to abnormal lung development [26]. The surviving adult mice have joint defects and tumorigenesis in the lung, skin, and liver [27–29] as well as features that resemble chronic obstructive pulmonary disease (COPD) [26]. *Mig-6* null mice also show accelerated lung AD when crossed with an *Egfr* mutant-driven transgenic mouse [30]. Moreover, airway ablation of *Mig-6* in combination with loss of the tumor suppressor gene, *Pten*, shows activated ERBB2 phosphorylation and the development of AD [31]. To investigate the role of *Mig-6* in *Kras*-driven lung cancer development *in vivo*, we crossed $Mig\text{-}6^{f/f}$ alleles into the *CCSP-Cre/LSL-*$Kras^{G12D}$ ($Kras^{G12D}$) background to generate $CCSP^{Cre}/LSL\text{-}Kras^{G12D}/Mig\text{-}6^{f/f}$ ($Mig\text{-}6^{d/d}Kras^{G12D}$) mice.

Results

Decreased MIG-6 expression in *Kras*^{G12D}-induced Mouse Lung Hyperplasia and Adenomas

The expression of MIG-6 was investigated in the tumors of *CCSP*^{Cre} *Kras*^{G12D} (Kras^{G12D}) mouse lungs. Immunostaining revealed that expression of MIG-6 protein was prominent in epithelia of normal airways, slightly reduced in hyperplastic lesions, and almost lost completely in adenomatous lesions (Fig. 1A). *Mig-6* mRNA levels were significantly reduced not only in the hyperplastic airways, but also in adenomatous lesions compared to normal airways (Fig.1B). The post-transcriptional modification may cause the differences between MIG-6 protein and its mRNA levels in hyperplastic airways. This discrepancy may also be due to the sensitivity of each assay. These results indicate that *Mig-6* expression is negatively correlated with lung cancer progression.

Mig-6 Deficiency Accelerated *Kras*^{G12D}-induced Mouse Lung Tumor Phenotypes

To determine the role of *Mig-6* in *Kras*^{G12D}-induced lung tumorigenesis, *Mig-6* was conditionally ablated in Club cells by breeding *Mig6*$^{f/f}$ mice to *CCSP*^{Cre}*Kras*^{G12D} mice, yielding *CCSP*^{Cre}*Mig-6*$^{d/d}$*Kras*^{G12D} mice (*Mig-6*$^{d/d}$*Kras*^{G12D}) [31]. *Mig-6*$^{d/d}$*Kras*^{G12D} mice had an average survival time of 18 weeks while *Kras*^{G12D} mice survived for an average time of 33 weeks (Fig. 2A). No mortality was observed in the *CCSP*^{Cre}*Mig-6*$^{f/f}$ (*Mig-6*$^{d/d}$) mice during this period (Fig. 2A). These results indicate that compound mutations of *Mig-6* deficiency and *Kras* activation imposed a severe negative impact on the health of the mice and shortened their life span.

Histological analysis of the lungs of 2-month-old *Mig-6*$^{d/d}$*Kras*^{G12D} mice revealed that *Mig-6*$^{d/d}$*Kras*^{G12D} mice developed severe airway hyperplasia and massive tumors throughout the lungs (Fig. 2B). *Mig-6*$^{d/d}$ mouse lungs exhibited no obvious morphological changes, while *Kras*^{G12D} mice exhibited prevalent hyperplasia surrounding airways compared with normal control animals (Fig. 2B). These results demonstrated that concomitant inactivation of *Mig-6* with *Kras*^{G12D} expression led to an early onset and robust progression of lung tumors.

To confirm the deletion of *Mig-6*, we examined genomic DNA isolated from the lungs of experimental mice. The lungs of global *Mig-6* knockout mice (*Mig-6*$^{-/-}$, a positive control) showed a 433 bp recombined band, whereas wild-type control lungs showed a 145 bp band (Sup. Fig. 1) [32]. At 1 month of age, we failed to detect the recombined *Mig-6* alleles in the *Mig-6*$^{d/d}$ and *Mig-6*$^{d/d}$*Kras*^{G12D} mouse lungs by PCR. By 4 months of age, the excised *Mig-6* allele was detected in *Mig-6*$^{d/d}$*Kras*^{G12D} lungs by PCR, but not in *Kras*^{G12D} lungs. These results suggest that the sensitivity of the PCR analysis was not able to detect the recombination in the 1-month old *Mig-6*$^{d/d}$ and *Mig-6*$^{d/d}$*Kras*^{G12D} mouse lungs due to contamination with the other lung cell types as well as Club cells without recombination at these loci. However, as tumor development progressed the number of cells with recombination at the *Mig-6* allele increased to a detectable level.

The pathology of *Mig-6* inactivation on the progression of *Kras*^{G12D}-induced lung tumors was quantified by scoring normal airways, hyperplastic lesions, atypical adenomatous hyperplasia (AAH), and adenomatous lesions in experimental mice up to 4 months of age.

Across all ages, *Mig-6*$^{d/d}$ and control lungs showed only normal airway morphology (Fig. 3). With *Kras*^{G12D}, animals exhibited less normal airways and more hyperplastic lesions, as early as, 1 month of age (Fig. 3A-B). Moreover, AAH and adenomatous lesions began to emerge at 2 months of age in *Kras*^{G12D} animals (Fig. 3C-D), indicating that cancer development is in progress [33]. Compared with the *Kras*^{G12D} animals, the *Mig-6*$^{d/d}$*Kras*^{G12D} mice had significantly more adenoma at 4 months of age (Fig. 3D) and increased presence of AAH across all ages (Fig. 3C) at the expense of normal airways (Fig. 3A). *Mig-6* deficiency and *Kras* activation jointly facilitated cancer progression, advancing all the diseased foci to become AAH and adenoma instead of hyperplastic lesions (Fig. 3B-D). Collectively, these results demonstrate that *Mig-6* inactivation greatly enhanced *Kras*^{G12D}–induced lung tumor progression.

Inflammation Was Enhanced in *Mig-6*$^{d/d}$*Kras*^{G12D} Mouse Lungs Compared to *Kras*^{G12D} Mouse Lungs

Inflammation has been shown to promote Kras mediated oncogenesis [34]. Our previous study showed that *Mig-6* null mice developed a COPD-like phenotype caused by recurrent inflammation [26], suggesting the role of *Mig-6* in inflammation. To determine whether *Mig-6* inactivation alters inflammatory responses during lung tumorigenesis, we examined the immune cell composition in bronchoalveolar lavage fluid (BALF) collected by lavaging lungs of experimental mice at 2 months of age. Consistent with histological findings, *Mig-6*$^{d/d}$ and control mice were comparable in both white blood cell (WBC) counts and expression levels of inflammatory markers (Fig. 4A). As expected, the *Kras*^{G12D} BALF exhibited statistically higher counts in total WBCs and lymphocytes and a trend of increase in neutrophils and macrophages compared with control and *Mig-6*$^{d/d}$ mice (Fig. 4A). Importantly, *Mig-6* deficiency further stimulated the inflammatory response in *Kras*^{G12D} mouse lungs, as demonstrated by the significantly increased numbers of WBCs, lymphocytes, and macrophages in *Mig-6*$^{d/d}$*Kras*^{G12D} BALF compared to *Kras*^{G12D} mice (Fig. 4A). Moreover, elevated pro-inflammatory genes including *Csf2, Mip1a, Il13a1, Tnfr2, Cox2*, and *Il18* were observed in *Mig-6*$^{d/d}$*Kras*^{G12D} lungs compared to those in *Kras*^{G12D} lungs (Fig. 4B). Notably, all these genes were shown to be associated with cancer inflammation and increased cancer risk [35–40]. Meanwhile, mucous cell metaplasia is a common phenomenon in lung inflammation and is also a feature for subtypes of lung AD [41]. To determine whether mucous cell metaplasia developed in *Mig-6*$^{d/d}$*Kras*^{G12D} lungs, we performed PAS staining in the lungs of experimental mice at 2 months of age [42]. As shown in Fig. 4C, we found metaplastic mucous cells in *Kras*^{G12D} lungs (black arrows), but not in control and *Mig-6*$^{d/d}$ mice. *Mig-6* deficiency in the *Kras* active background further increased the number of metaplastic mucous cells in comparison with that in *Kras*^{G12D} mice (Fig. 4C). To confirm the results from PAS staining, we examined the mRNA levels of *Muc5ac,* a marker gene in the lung mucous cell metaplasia [42]. Consistent with the PAS staining results, *Mig-6* inactivation greatly increased the expression of *Muc5ac* in the *Kras*^{G12D} background (Fig. 4D). Although those analyses don't directly prove that this increased inflammation promoted tumor development in *Mig-6*$^{d/d}$*Kras*^{G12D} mice, these results showed inflammation was enhanced in *Mig-6*$^{d/d}$*Kras*^{G12D} lungs compared to *Kras*^{G12D} lungs, suggesting that this is a potential mechanism to explain the enhanced

tumorigenesis in *Mig-6*$^{d/d}$*Kras*^{G12D} lungs based on previous findings of inflammation promoting *Kras* mediated lung tumorigenesis [34].

Ablation of *Mig-6* Reduced Apoptosis in *Kras*^{G12D}-driven Tumors

In order to determine if the accelerated tumorigenesis as a result of *Mig6* deletion was due to an inhibition of apoptosis or an increase in cell proliferation, we assayed mouse lungs utilizing TUNEL staining and phospho-histone H3 staining, respectively, at 1 month of age. Figure 5 shows that while *Kras*^{G12D} had an increase in apoptosis, *Mig-6*$^{d/d}$*Kras*^{G12D} lungs show similar apoptotic levels as control and *Mig-6*$^{d/d}$ mice (Fig. 5A-B). On the other hand, the number of proliferative cells in *Mig-6*$^{d/d}$*Kras*^{G12D} lungs was significantly more than that in the control and *Mig-6*$^{d/d}$ lungs (Fig. 5C-D), whereas there was no significant difference between *Kras*^{G12D} and *Mig-6*$^{d/d}$*Kras*^{G12D} lungs (Fig. 5D). These results suggest that *Mig-6* deficiency promotes cell survival by reducing apoptosis in *Kras*^{G12D} mouse lungs, while it does not affect cell proliferation in this *Kras* dependent lung tumor mouse model. To further demonstrate that *MIG-6* deficiency attenuates the apoptosis in pulmonary epithelial cells with *KRAS*^{G12D} expression, *MIG-6* was ablated by the CRISPR/Cas9 technology in A427 cells, a human lung adenocarcinoma cell line expressing *KRAS*^{G12D}, followed by Cisplatin challenge to induce apoptosis. As shown in Figure 5E, cleaved-PARP, a marker of apoptosis, exhibited lower levels in the *MIG-6* ablated cells compared with that in control groups, especially under Cisplatin challenge. This finding indicates that *MIG-6* deficiency suppresses apoptosis in human KRAS-active AD cells, which is the consistent with the apoptosis-attenuating capacity of *Mig-6* deficiency in mouse lung AD. Taken together, our data reveal that *Mig-6* is an important positive regulator of apoptosis in lung KRAS-active AD cells (Fig. 5).

ErbB4 Pathway Was Activated in MIG-6 Deficient, KRAS Active Lung Tumor and Attenuated Apoptosis

Based on the findings that *Mig-6* suppresses *EGFR, AKT and mTOR* signaling pathways [26], we examined the total and phosphorylated protein levels of the EGFR family, AKT and mTOR in lungs and lung tumors of 2-month old mice using Western blot and immunohistochemical analysis. As shown in Fig. 6A-B and Sup. Fig. 2A-F, the phosphorylation of all ERBB proteins was increased after ablation of *Mig-6* in wild type mouse lung. However, only the phosphorylation of ERBB4 was increased when *Mig-6* was deleted in the *Kras*^{G12D} mouse lungs (Fig. 6A-B). Additionally, ERBB4 protein was also increased in *Kras*^{G12D} and *Mig-6*$^{d/d}$*Kras*^{G12D} mouse lungs compared to wild type mouse lungs (Fig. 6A-B), indicating that ErbB4 pathway was activated in the *Mig-6*$^{d/d}$ *Kras*^{G12D} mice by the increase of its phosphorylation and total protein.

To assess whether the increased ERBB4 phosphorylation is due to *Mig-6* ablation in KRAS active AD cells, we examined p-ERBB4 levels in *MIG-6* knock-out A427 cells. As shown in Fig. 6C, p-ERBB4 levels were increased after knock-out of *MIG-6*, demonstrating a conserved role of MIG-6 in regulation of p-ERBB4 in lung tumors expressing *KRAS*^{G12D} between mouse and human. Next we examine whether ErbB4 pathway may alter apoptosis in lung adenoma of *Mig-6*$^{-/-}$*Kras*^{G12D} background. By ablating *ERBB4* in A427 cells that have *MIG-6* deficiency and constitutive *KRAS*^{G12D} expression, *ERBB4* ablation showed

increased cell apoptosis with or without the treatment of Cisplatin (Fig. 6D). This finding demonstrates the activation of the ErbB4 pathway suppressed apoptosis in MIG-6 deficient, KRAS active lung AD cells.

Interestingly, we did not detect differences on mTOR phosphorylation levels between *Kras*^{G12D} and *Mig-6*$^{d/d}$*Kras*^{G12D} mouse lung tumors (Sup. Fig. 2G), and AKT phosphorylation levels were very low in both *Kras*^{G12D} and *Mig-6*$^{d/d}$*Kras*^{G12D} mouse lung tumors (Sup. Fig. 2H) despite the fact that AKT is often activated by *EGFR* signaling [43]. Our results are consistent with a previous report that AKT phosphorylation is not increased in response to activated *Kras*-induced mouse lung tumors [44]. In summary, our results suggest that the ErbB4 pathway is activated in MIG-6 deficient, KRAS active lung AD cells to prevent apoptosis.

Discussion

In the present study, we showed that *Mig-6* ablation in Club cells enhanced *Kras*^{G12D}-driven mouse lung tumorigenesis through suppressing the cell apoptosis in *Kras*^{G12D} mouse lungs partially by activation of the ErbB4 pathway.

ERBB4 is mutated in 5.4% of NSCLC patients [45]. ERBB4 overexpression is correlated with Tumor, Lymph node, and Metastasis (TNM) staging and decreased survival after operations in NSCLC patients [46]. It is well documented that *Mig-6* is a negative regulator of *ErbB* signaling and *Mig-6* expression is closely associated with *ErbB* signaling in lung cancers [30, 31, 47–49]. Although p-EGFR has been reported to be a major ERBB member regulated by MIG-6 [20], surprisingly only p-ErbB4 levels, instead of p-EGFR levels, were significantly increased after ablation of *Mig-6* in *Kras*^{G12D} mouse lungs and ERBB4 protein was also increased in *Kras*^{G12D} and *Mig-6*$^{d/d}$*Kras*^{G12D} mouse lungs compared to wild type mouse lungs. Previous studies have demonstrated that ERBB4 mutants (Y285C, D595V, D931Y and K935I) increase both basal and ligand-induced ERBB4 phosphorylation and promote NIH 3T3 cell survival under serum starvation, probably by sustaining their own phosphorylation status [45]. Moreover, *ERBB4* has been shown to promote human lung cancer cell proliferation [50] as well as exhibits oncogenic activities in both breast cancer cells [51, 52] and pancreatic tumor cell lines [53]. These results collectively suggest that the activated ErbB4 pathway could be a potential mechanism to explain how *Mig-6* affects *Kras*-mutant-driven lung tumor development. Indeed, we observed a remarkable decrease of cell apoptosis in *Mig-6*$^{d/d}$*Kras*^{G12D} lungs, with the elevated phosphorylated ERBB4 levels, compared to those in *Kras*^{G12D} lungs at the early stage of tumor formation. Functional assessment on A427 cells further showed the role of MIG-6 and ERBB4 in regulation of apoptosis. Given that inhibition of cell apoptosis may be the major advantage that tumor cells gained upon loss of MIG-6 [54], the increased *ErbB4* signaling, in response to MIG-6 deficiency, likely serves as a major downstream effector for MIG-6 to regulate cell apoptosis. Further studies are needed to help understand how the *ErbB4* pathway regulates apoptosis in lung cancer.

The inflammatory response was also impacted in lung tumor progression in *Mig-6*$^{d/d}$*Kras*^{G12D} mice. Our previous study showed that *Mig-6* null mice developed a

COPD-like phenotype that was accompanied by increased macrophage invasion and mucous cell metaplasia [26]. In agreement with the previous findings, we observed a significant increase in inflammatory cell number in the BALF, as well as, upregulated expression of tumor inflammation-associated genes in *Mig-6*$^{d/d}$*Kras*^{G12D} lungs compared to *Kras*^{G12D} lungs. In addition, *Mig-6*$^{d/d}$*Kras*^{G12D} mice also exhibited increased mucous cell metaplasia in the airways, another indication of increased inflammation associated with *Mig-6* inactivation in comparison with those of *Kras*^{G12D} mice. In the present study, it is difficult to determine the causal relationship between the increased inflammatory responses and lung tumor development. However, inflammation has been shown to promote *Kras* mediated lung tumorigenesis [34], suggesting that heightened inflammation may contribute to enhanced tumor progression.

It is well documented that *MIG-6* expression is decreased in several human cancers [48, 49, 55]. Our previous work shows that MIG-6 levels decrease during the development of lung adenosquamous induced by *Pten* and *Smad4* ablation [31]. In the present study, we also found decreased *Mig-6* expression in hyperplastic and adenomatous lesions in *Kras*^{G12D} mouse lungs. Previous findings have demonstrated that the expression level of MIG-6 is reduced in human lung adenocarcinoma A427 cells having *KRAS*^{G12D} due to epigenetic silencing of *MIG-6* through methylation and histone deacetylation without having a physical alteration in its promoter [56]. The relationship between MIG-6 expression and KRAS activation may be an indication of how the pro-oncogenic signaling caused by *Kras* mutation suppresses inhibitors of tumor progression and provides enhanced growth advantages for the transformed cells while the loss of *Mig-6* provides a selective advantage for tumor cell growth. Therefore, it is important to understand how tumor suppressors, such as MIG-6, are inhibited during cancer development. This will provide new avenues for the treatment of lung cancer.

Besides *Mig-6* preventing *Kras*^{G12D}-driven lung tumor progression as reported in the present study, these two genes are also implicated in cancer cell sensitivity to drug treatment [18]. LOVO (colorectal AD) and SNU668 (gastric AD) cells carry mutant *KRAS* and are sensitive to MEK inhibition. Interestingly, down-regulation of *Mig-6* confers LOVO and SNU668 cell resistance to MEK inhibition. In contrast, overexpression of *Mig-6* re-sensitizes the cells to MEK inhibition while mutant *Kras* positive parental HCT116 (colorectal AD) and AGS (gastric AD) cells are resistant to MEK inhibition [18]. Meanwhile, Sun *et al.* showed that transcriptional induction of ERBB3 caused the resistance to MEK inhibition in *KRAS* mutant lung and colon cancer [57]. These findings collectively suggest that targeting the oncogenic pathway regulated by MIG-6, such as the ERBB4 pathway, might be key to effective treatment of *KRAS*-driven lung tumors since there is no FDA approved drug specific for treatment of lung cancer patients having *KRAS* mutations.

In summary, we developed genetically engineered mouse lung tumor models and revealed the role of *Mig-6* inactivation in promoting *Kras*^{G12D}-driven lung tumor development by attenuating apoptosis in *Kras*^{G12D} mouse lungs, which is partially through elevated *ErbB4* signaling. This discovery provides a new direction to develop novel preventive and/or therapeutic strategies (e.g., restoration of Mig-6 expression or inhibition of the ErbB4 pathway) for treating *KRAS*-mutant-driven lung cancer in patients.

Materials and Methods

Animals, BALF, and Histology

All the animal protocols are approved by the National Institute of Environmental Health Sciences and the Baylor College of Medicine. All experiments were conducted in accordance with relevant guidelines and regulations of both institutions. Bronchoalveolar lavage fluid (BALF) was collected by lavaging lungs of mice with 2 ml PBS. Total leukocytes were counted with a hemocytometer and differential inflammatory cells were counted from cytocentrifuged BALF (100 μl) followed with Wright-Giemsa staining [58]. Hematoxylin and eosin (H&E) and Periodic Acid Schiff (PAS) staining were performed according to previous protocols [31].

Laser Capture Microdissection

Laser capture was performed according to standard protocols by using the Arcturus PixCell II Microdissection system (www.arcturus.com) with the following parameters being utilized: laser spot size 7.5 um, pulse power 50 mW, pulse width 0.75 ms and a threshold voltage of 205 mV.

Cell line and culture

A427 cells (ATCC® HTB-53™) were purchased from ATCC and cultured in ATCC-formulated Eagle's Minimum Essential Medium (Cat. 30-2003) following the culture method of ATCC. 20 μM Cisplatin was used to treat A427 cells for 0h, 12h and 24h, at which time cells were collected for protein analysis.

Immunofluorescence (IF) staining, immunohistochemistry (IHC) and Western Blot (WB)

IF, IHC and WB were performed as previously described [31]. The following primary antibodies were used: anti-*Mig-6* (MilliporeSigma, Billerica, MA), anti-p-Histone H3 (MilliporeSigma, Billerica, MA), anti-CCSP (DeMayo lab), anti-pro-SP-C (Seven Hills Bioreagents, Cincinnati, OH), anti-p-EGFR (CST3777), anti-p-EGFR (sc-12351), anti-EGFR (CST4267), anti-p-ERBB2 (sc-293110), anti-ERBB2 (sc-284), anti-p-ERBB3 (CST4791), anti-ERBB3 (sc-285), anti-p-ERBB4 (ab92782 and sc-33040), anti-ERBB4 (CST4795 and sc-283) (Santa Cruz Biotechnologies, Dallas, TX), anti-PARP (CST 9542), anti-MIG-6 (DeMayo lab), anti-AKT (CST4691), anti-p-AKT (CST4060), p-mTOR (CST 2971), and anti-mTOR (CST2983). Cisplatin (22-515-0) was purchased from ThermoFisher Scientific, Waltham, MA.

Cell proliferation and apoptosis analysis

Cell proliferation was assayed with phospho-Histone H3 immunohistochemistry as described above and apoptotic cells were detected with the *In Situ* Cell Death Detection Kit (Roche, Mannheim, Germany) following the instructions of the manufacturer.

Quantitative Real-time PCR

Quantitative Real-time PCR was performed as previously described [31]. All the primers and Taqman probes were purchased from Applied Biosystems/ThermoFisher Scientific (Waltham, MA).

Lentiviral CRISPR/Cas9-gRNA targeting human MIG-6 and ERBB4

The sequences of gRNA targeting *MIG-6* and *ERBB4* are "CTCGGTGTGCGCGAGTTACT" and "TTATGAGGATCGATATGCCT", respectively. These gRNAs were cloned into LentiCRISPRv2 vector [59] by GenScript (Piscataway, NJ). CRISPR-Lenti non-targeting control plasmid was purchased from MilliporeSigma (Billerica, MA) (CRISPR12-1EA) and its sequences of gRNA is "CGCGATAGCGCGAATATATT". Lentiviruses were made in the Viral Vector Core Laboratory of NIH/NIEHS and then were used to infect A427 cells for knocking out *MIG-6* and *ERBB4*. The pooled cells infected by gRNA were collected for WB to confirm the knockout efficiency. Non-infected and gRNA-Control-infected cells were used as controls.

Statistics

Measurement values are expressed as mean ± SE (standard error). Student's *t* test was used for comparison of two group averages. When there were more than two groups, One-way ANOVA followed by Tukey's analysis was performed. All the Ns were ≥3 and statistically significance was considered when *P* values were ≤ 0.05.

Supplementary Material

Refer to Web version on PubMed Central for supplementary material.

Acknowledgments

We thank Jinghua Li, Bryan Ngo, Jie Yang, and Janet DeMayo, M.S. for technical assistance; Janet DeMayo, M.S., Weiwen Long, Ph.D. and Heather Franco, Ph.D. for manuscript preparation. This research is supported by the Intramural Research Program of the National Institute of Environmental Health Sciences Project Z1AES103311-01 (F.J.D.) and by the National Cancer Institute Grant U01CA105352 (F.J.D.).

References

1. Landis SH, et al. Cancer statistics, 1999. CA: a cancer journal for clinicians. 1999; 49(1):8–31. 1. [PubMed: 10200775]
2. Kwon MC, Berns A. Mouse models for lung cancer. Molecular oncology. 2013; 7(2):165–77. [PubMed: 23481268]
3. van Zandwijk N, Mooi WJ, Rodenhuis S. Prognostic factors in NSCLC. Recent experiences. Lung cancer. 1995; (12 Suppl 1):S27–33. [PubMed: 7551931]
4. Schiller JH. Current standards of care in small-cell and non-small-cell lung cancer. Oncology. 2001; (61 Suppl 1):3–13. [PubMed: 11598409]
5. Walker S. Updates in non-small cell lung cancer. Clin J Oncol Nurs. 2008; 12(4):587–96. [PubMed: 18676326]
6. Jemal A, et al. Cancer statistics, 2010. CA Cancer J Clin. 2010; 60(5):277–300. [PubMed: 20610543]
7. Travis WD. Pathology of lung cancer. Clinics in chest medicine. 2002; 23(1):65–81. viii. [PubMed: 11901921]

8. Ding L, et al. Somatic mutations affect key pathways in lung adenocarcinoma. Nature. 2008; 455(7216):1069–75. [PubMed: 18948947]
9. Slebos RJ, Rodenhuis S. The ras gene family in human non-small-cell lung cancer. Journal of the National Cancer Institute. Monographs. 1992; (13):23–9. [PubMed: 1327034]
10. Sanders HR, Albitar M. Somatic mutations of signaling genes in non-small-cell lung cancer. Cancer genetics and cytogenetics. 2010; 203(1):7–15. [PubMed: 20951313]
11. Campbell SL, et al. Increasing complexity of Ras signaling. Oncogene. 1998; 17(11 Reviews): 1395–413. [PubMed: 9779987]
12. Tsutsumi K, et al. Visualization of Ras-PI3K interaction in the endosome using BiFC. Cellular signalling. 2009; 21(11):1672–9. [PubMed: 19616621]
13. Wang XQ, et al. Oncogenic K-Ras regulates proliferation and cell junctions in lung epithelial cells through induction of cyclooxygenase-2 and activation of metalloproteinase-9. Molecular biology of the cell. 2009; 20(3):791–800. [PubMed: 19037103]
14. Singh A, et al. TAK1 inhibition promotes apoptosis in KRAS-dependent colon cancers. Cell. 2012; 148(4):639–50. [PubMed: 22341439]
15. Ji H, et al. K-ras activation generates an inflammatory response in lung tumors. Oncogene. 2006; 25(14):2105–12. [PubMed: 16288213]
16. Okada F, et al. Impact of oncogenes in tumor angiogenesis: mutant K-ras up-regulation of vascular endothelial growth factor/vascular permeability factor is necessary, but not sufficient for tumorigenicity of human colorectal carcinoma cells. Proceedings of the National Academy of Sciences of the United States of America. 1998; 95(7):3609–14. [PubMed: 9520413]
17. Meuwissen R, Berns A. Mouse models for human lung cancer. Genes Dev. 2005; 19(6):643–64. [PubMed: 15769940]
18. Yoon YK, et al. Down-regulation of mitogen-inducible gene 6, a negative regulator of EGFR, enhances resistance to MEK inhibition in KRAS mutant cancer cells. Cancer letters. 2012; 316(1): 77–84. [PubMed: 22082529]
19. Zhang YW, Vande Woude GF. Mig-6, signal transduction, stress response and cancer. Cell cycle. 2007; 6(5):507–13. [PubMed: 17351343]
20. Anastasi S, et al. Regulation of the ErbB network by the MIG6 feedback loop in physiology, tumor suppression and responses to oncogene-targeted therapeutics. Semin Cell Dev Biol. 2016; 50:115–24. [PubMed: 26456277]
21. Anastasi S, et al. Loss of RALT/MIG-6 expression in ERBB2-amplified breast carcinomas enhances ErbB-2 oncogenic potency and favors resistance to Herceptin. Oncogene. 2005; 24(28): 4540–8. [PubMed: 15856022]
22. Li Z, et al. Downregulation of Mig-6 in nonsmall-cell lung cancer is associated with EGFR signaling. Molecular carcinogenesis. 2012; 51(7):522–34. [PubMed: 21739478]
23. Jeong JW, et al. Mig-6 modulates uterine steroid hormone responsiveness and exhibits altered expression in endometrial disease. Proceedings of the National Academy of Sciences of the United States of America. 2009; 106(21):8677–82. [PubMed: 19439667]
24. Lin CI, et al. Mitogen-inducible gene-6 is a multifunctional adaptor protein with tumor suppressor-like activity in papillary thyroid cancer. The Journal of clinical endocrinology and metabolism. 2011; 96(3):E554–65. [PubMed: 21190978]
25. Ying H, et al. Mig-6 controls EGFR trafficking and suppresses gliomagenesis. Proceedings of the National Academy of Sciences of the United States of America. 2010; 107(15):6912–7. [PubMed: 20351267]
26. Jin N, et al. Mig-6 is required for appropriate lung development and to ensure normal adult lung homeostasis. Development. 2009; 136(19):3347–56. [PubMed: 19710174]
27. Zhang YW, et al. Evidence that MIG-6 is a tumor-suppressor gene. Oncogene. 2007; 26(2):269–76. [PubMed: 16819504]
28. Ferby I, et al. Mig6 is a negative regulator of EGF receptor-mediated skin morphogenesis and tumor formation. Nature medicine. 2006; 12(5):568–73.
29. Reschke M, et al. Mitogen-inducible gene-6 is a negative regulator of epidermal growth factor receptor signaling in hepatocytes and human hepatocellular carcinoma. Hepatology. 2010; 51(4): 1383–90. [PubMed: 20044804]

30. Maity TK, et al. Loss of MIG6 Accelerates Initiation and Progression of Mutant Epidermal Growth Factor Receptor-Driven Lung Adenocarcinoma. Cancer Discov. 2015; 5(5):534–49. [PubMed: 25735773]
31. Liu J, et al. ErbB2 Pathway Activation upon Smad4 Loss Promotes Lung Tumor Growth and Metastasis. Cell Rep. 2015
32. Jin N, et al. Generation of a Mig-6 conditional null allele. Genesis. 2007; 45(11):716–21. [PubMed: 17987665]
33. Moghaddam SJ, et al. Promotion of lung carcinogenesis by chronic obstructive pulmonary disease-like airway inflammation in a K-ras-induced mouse model. Am J Respir Cell Mol Biol. 2009; 40(4):443–53. [PubMed: 18927348]
34. Kitajima S, Thummalapalli R, Barbie DA. Inflammation as a driver and vulnerability of KRAS mediated oncogenesis. Semin Cell Dev Biol. 2016; 58:127–35. [PubMed: 27297136]
35. He JQ, et al. Association of genetic variations in the CSF2 and CSF3 genes with lung function in smoking-induced COPD. The European respiratory journal : official journal of the European Society for Clinical Respiratory Physiology. 2008; 32(1):25–34.
36. Koch AE, et al. Macrophage inflammatory protein-1 alpha. A novel chemotactic cytokine for macrophages in rheumatoid arthritis. The Journal of clinical investigation. 1994; 93(3):921–8. [PubMed: 8132778]
37. Rothenberg ME, et al. IL-13 receptor alpha1 differentially regulates aeroallergen-induced lung responses. Journal of immunology. 2011; 187(9):4873–80.
38. Mizoguchi E, et al. Role of tumor necrosis factor receptor 2 (TNFR2) in colonic epithelial hyperplasia and chronic intestinal inflammation in mice. Gastroenterology. 2002; 122(1):134–44. [PubMed: 11781288]
39. Seibert K, Masferrer JL. Role of inducible cyclooxygenase (COX-2) in inflammation. Receptor. 1994; 4(1):17–23. [PubMed: 8038702]
40. Rovina N, et al. Interleukin-18 in induced sputum: association with lung function in chronic obstructive pulmonary disease. Respiratory medicine. 2009; 103(7):1056–62. [PubMed: 19208460]
41. Nikitin AY, et al. Classification of proliferative pulmonary lesions of the mouse: recommendations of the mouse models of human cancers consortium. Cancer research. 2004; 64(7):2307–16. [PubMed: 15059877]
42. Curran DR, Cohn L. Advances in mucous cell metaplasia: a plug for mucus as a therapeutic focus in chronic airway disease. American journal of respiratory cell and molecular biology. 2010; 42(3):268–75. [PubMed: 19520914]
43. Bliesath J, et al. Combined inhibition of EGFR and CK2 augments the attenuation of PI3KAkt-mTOR signaling and the killing of cancer cells. Cancer Lett. 2012; 322(1):113–8. [PubMed: 22387988]
44. Xu C, et al. Loss of Lkb1 and Pten leads to lung squamous cell carcinoma with elevated PD-L1 expression. Cancer Cell. 2014; 25(5):590–604. [PubMed: 24794706]
45. Kurppa KJ, et al. Activating ERBB4 mutations in non-small cell lung cancer. Oncogene. 2016; 35(10):1283–91. [PubMed: 26050618]
46. Deng Z, et al. [A study on the expression of erbB4/HER4 in non-small cell lung cancer]. Zhongguo Fei Ai Za Zhi. 2002; 5(3):177–9. [PubMed: 21324275]
47. Hackel PO, Gishizky M, Ullrich A. Mig-6 is a negative regulator of the epidermal growth factor receptor signal. Biol Chem. 2001; 382(12):1649–62. [PubMed: 11843178]
48. Ferby I, et al. Mig6 is a negative regulator of EGF receptor-mediated skin morphogenesis and tumor formation. Nat Med. 2006; 12(5):568–73. [PubMed: 16648858]
49. Li Z, et al. Downregulation of Mig-6 in nonsmall-cell lung cancer is associated with EGFR signaling. Mol Carcinog. 2012; 2011(7):20815.
50. Starr A, et al. ErbB4 increases the proliferation potential of human lung cancer cells and its blockage can be used as a target for anti-cancer therapy. Int J Cancer. 2006; 119(2):269–74. [PubMed: 16463386]
51. Mill CP, et al. ErbB2 Is Necessary for ErbB4 Ligands to Stimulate Oncogenic Activities in Models of Human Breast Cancer. Genes Cancer. 2011; 2(8):792–804. [PubMed: 22393464]

52. Haskins JW, Nguyen DX, Stern DF. Neuregulin 1-activated ERBB4 interacts with YAP to induce Hippo pathway target genes and promote cell migration. Sci Signal. 2014; 7(355):ra116. [PubMed: 25492965]

53. Mill CP, Gettinger KL, Riese DJ 2nd. Ligand stimulation of ErbB4 and a constitutively-active ErbB4 mutant result in different biological responses in human pancreatic tumor cell lines. Exp Cell Res. 2011; 317(4):392–404. [PubMed: 21110957]

54. Kim TH, et al. The synergistic effect of Mig-6 and Pten ablation on endometrial cancer development and progression. Oncogene. 2010; 29(26):3770–80. [PubMed: 20418913]

55. Amatschek S, et al. Tissue-wide expression profiling using cDNA subtraction and microarrays to identify tumor-specific genes. Cancer Res. 2004; 64(3):844–56. [PubMed: 14871811]

56. Zhang YW, et al. Cancer-type regulation of MIG-6 expression by inhibitors of methylation and histone deacetylation. PLoS One. 2012; 7(6):e38955. [PubMed: 22701735]

57. Sun C, et al. Intrinsic resistance to MEK inhibition in KRAS mutant lung and colon cancer through transcriptional induction of ERBB3. Cell Rep. 2014; 7(1):86–93. [PubMed: 24685132]

58. Strober, W. Wright-Giemsa and nonspecific esterase staining of cells. In: Coligan, John E., et al., editors. Current protocols in immunology. 2001. Appendix 3: p. Appendix 3C

59. Sanjana NE, Shalem O, Zhang F. Improved vectors and genome-wide libraries for CRISPR screening. Nat Methods. 2014; 11(8):783–4. [PubMed: 25075903]

60. Chatterjee S, et al. Quantitative immunohistochemical analysis reveals association between sodium iodide symporter and estrogen receptor expression in breast cancer. PLoS One. 2013; 8(1):e54055. [PubMed: 23342072]

Highlights

- *Mig-6* deficiency promotes the development of $Kras^{G12D}$-induced mouse lung adenoma.
- *MIG-6* deficiency attenuates apoptosis of lung adenoma expressing $KRAS^{G12D}$.
- Total and phosphorylated ERBB4 is increased in adenoma of $Mig\text{-}6^{d/d}Kras^{G12D}$ lung.
- Ablation of ERBB4 increases apoptosis of lung adenocarcinoma cells ($MIG\text{-}6^{-/-}KRAS^{G12D}$).

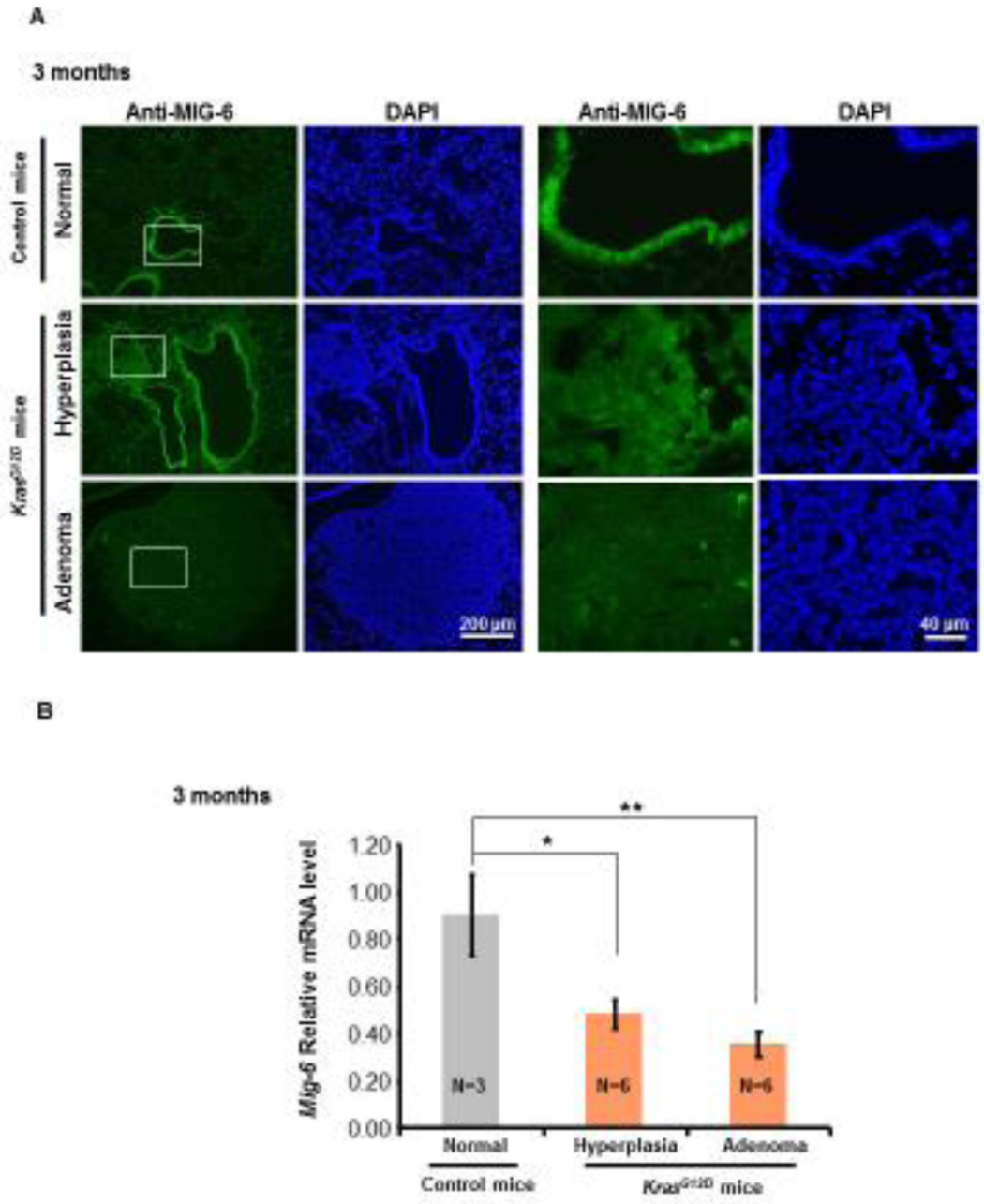

Figure 1. *Mig-6* expression was down-regulated in oncogenic *Kras*-induced (*CCSP*^{Cre}*Kras*^{G12D}) mouse lung tumors

(A) Representative immunofluorescent (IF) staining of *Mig-6* in normal airways of *LSL-Kras*^{G12D} mice and in hyperplastic lesions and adenomatous lesions *of Kras*^{G12D} mice (3 months of age). Three control mice and six *Kras*^{G12D} mice were used for IF staining and whole lungs were examined. One representative region for each group was chosen to present here. Regions in the white boxes were further magnified. (B) RT-qPCR analysis of *Mig-6* mRNA levels in Laser Capture Micro-dissected normal airways from the control mice (*LSL-Kras*^{G12D}) and hyperplastic lesions and adenomatous lesions from the lungs of *Kras*^{G12D} mice. (*p<0.05 and **p<0.01 vs. normal airways) (3 months of age).

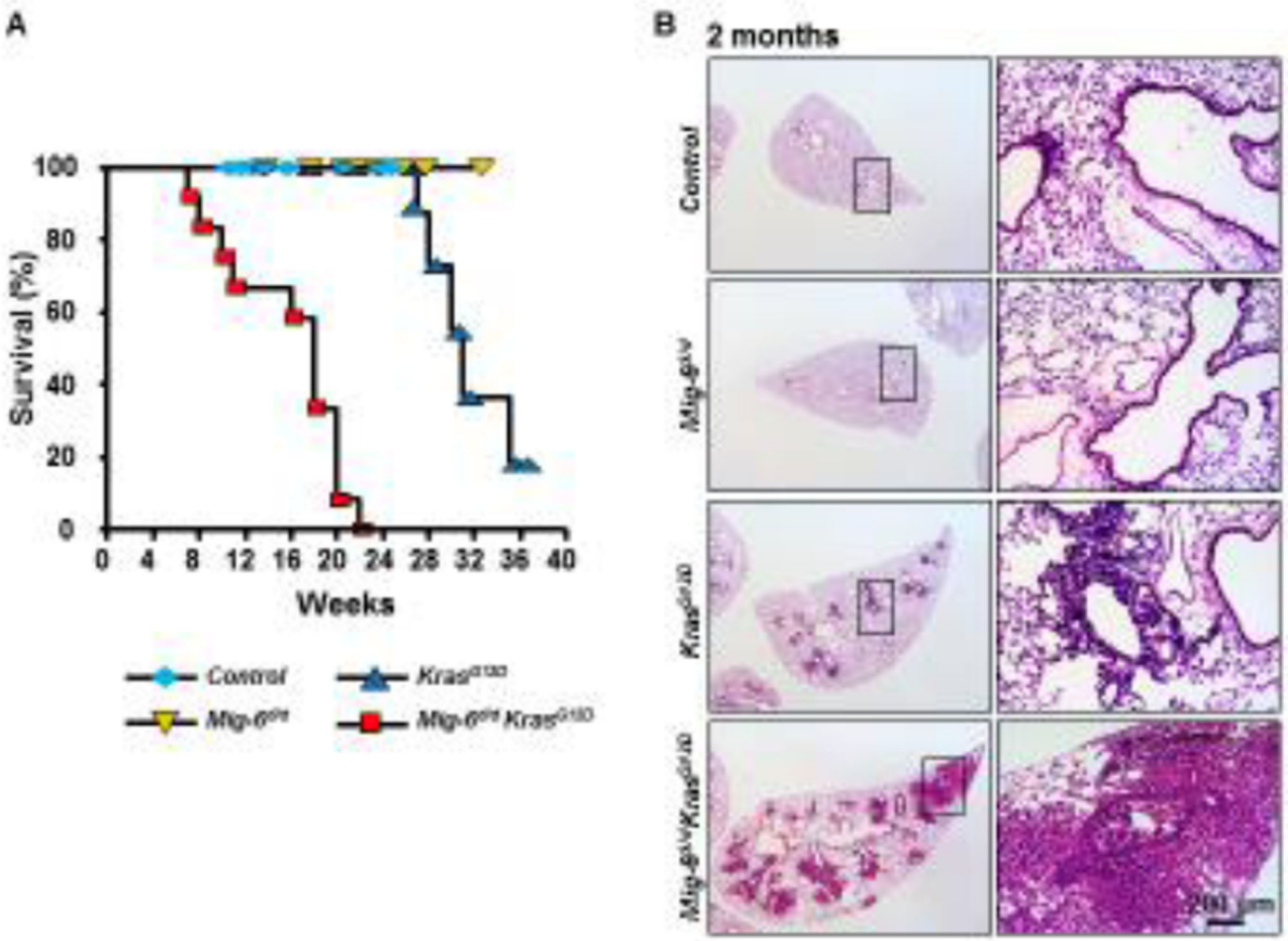

Figure 2. Reduced life span and increased lung neoplasia in *Mig-6*$^{d/d}$*Kras*^{G12D} mice

(A) Kaplan-Meier survival curves of control (*Mig-6*$^{f/f}$ or *LSL-Kras*^{G12D}), *Mig-6*$^{d/d}$, *Kras*^{G12D}, and *Mig-6*$^{d/d}$*Kras*^{G12D} mice (N=12 per each group). (B) H&E staining of lung tissues of control, *Mig-6*$^{d/d}$, *Kras*^{G12D}, and *Mig-6*$^{d/d}$*Kras*^{G12D} mice at the age of 2 months. Regions in black boxes were further magnified and shown in the right panels.

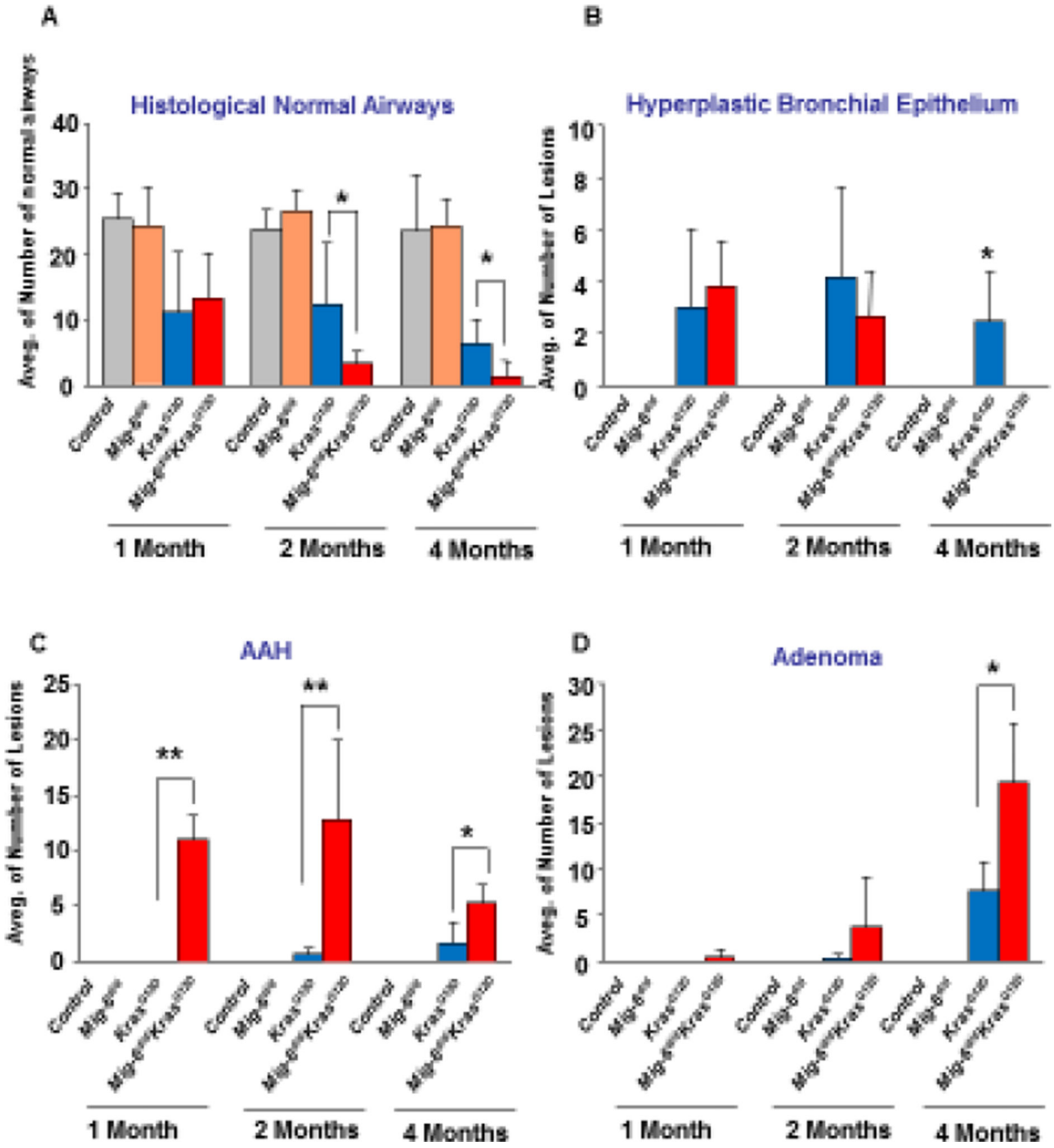

Figure 3. *Mig-6* inactivation enhanced histopathological changes during $Kras^{G12D}$–induced lung tumor progression

Histopathological changes were scored in H&E stained sections of the lungs of control, $Mig\text{-}6^{d/d}$, $Kras^{G12D}$, and $Mig\text{-}6^{d/d}Kras^{G12D}$ mice (at the age of 1, 2, and 4 months). Three mice were used for each group. Average numbers of normal airways (A), hyperplastic bronchial epithelium (B), Atypical Adenomatous Hyperplasia (AAH) (C), and adenomas (D) were calculated and shown in bar graphs. Independent pathologists counted and defined these histopathological patterns microscopically. *p<0.05 and **p<0.01 by One Way ANOVA followed by Tukey's analysis.

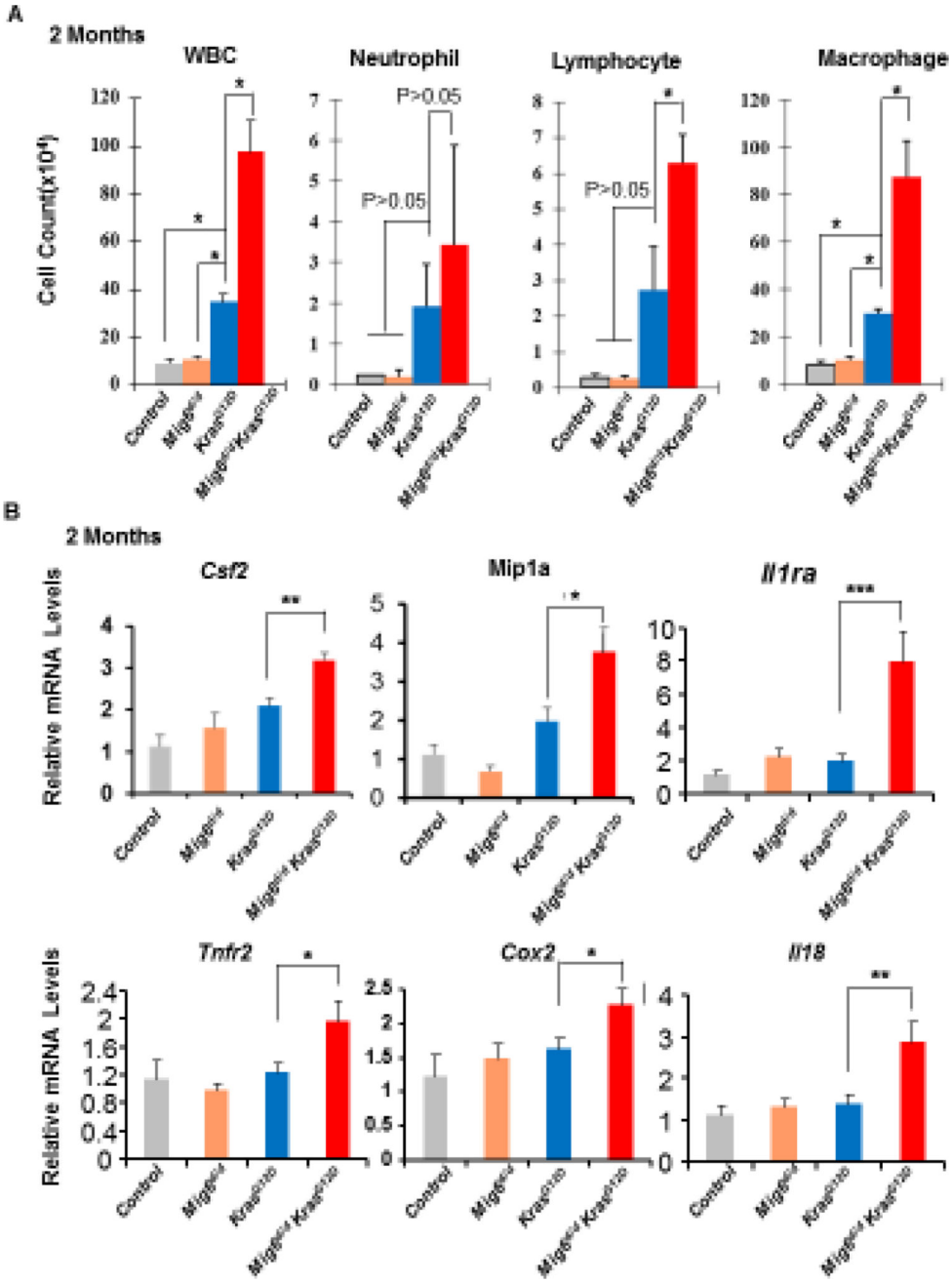

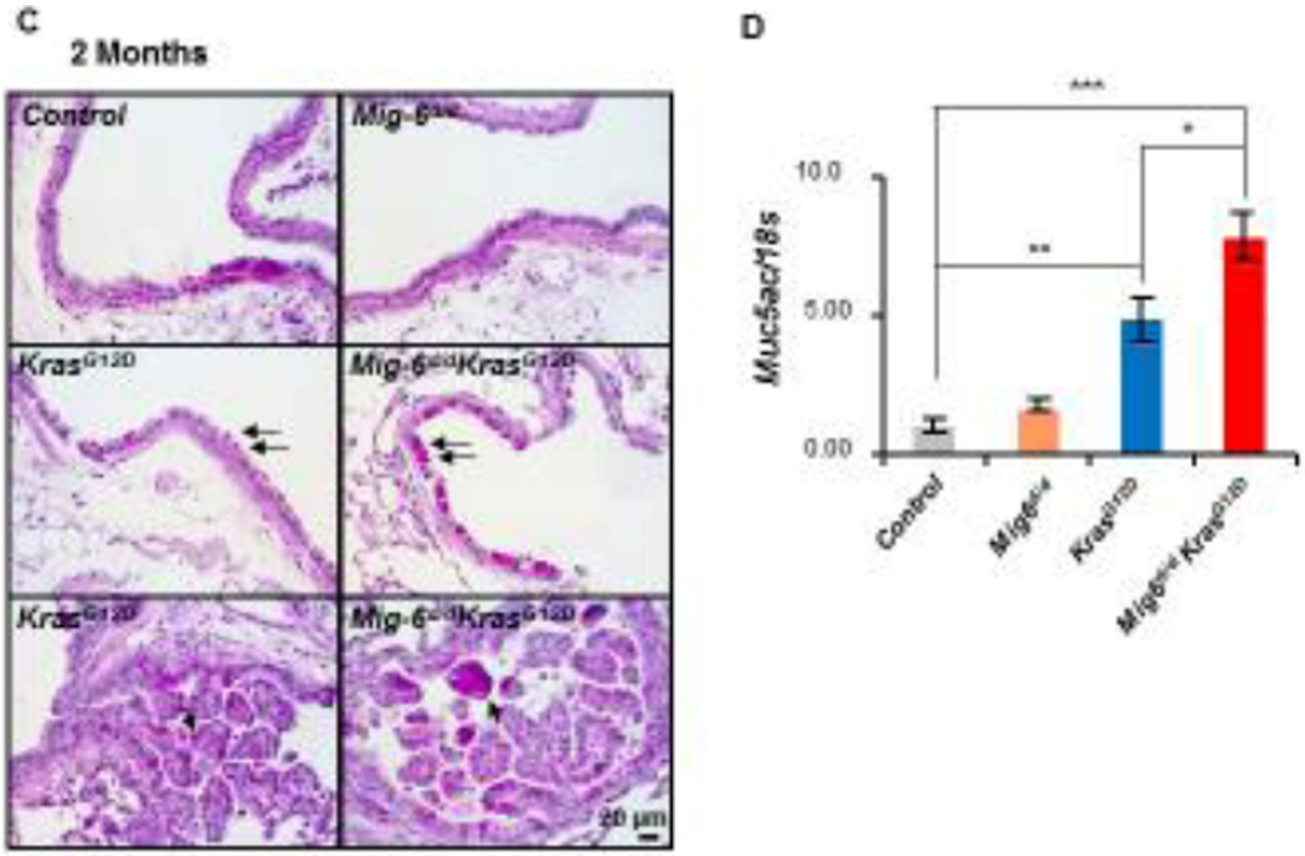

Figure 4. Inflammation was enhanced in *Mig-6*$^{d/d}$*Kras*^{G12D} mouse lungs

(A) Analysis of white blood cells (WBC), neutrophils, lymphocytes, and macrophages in the BALF of control, *Mig-6*$^{d/d}$, *Kras*^{G12D}, and *Mig-6*$^{d/d}$*Kras*^{G12D} mice, *P<0.05. Three mice were used for each group. (B) RT-qPCR analysis of the expression of pro-inflammatory genes in the lungs of control, *Mig-6*$^{d/d}$, *Kras*^{G12D}, and *Mig-6*$^{d/d}$*Kras*^{G12D} mice. * p<0.05, ** p<0.01 and *** p<0.001. (C) PAS staining of lungs of control, *Mig-6*$^{d/d}$, *Kras*^{G12D}, and *Mig-6*$^{d/d}$*Kras*^{G12D} mice (2 months of ages). Arrows indicate metaplastic mucus cells in the bronchial epithelium. (D) RT-qPCR analysis of mRNA levels of *Muc5ac* in the lungs of mice (2 months of age). * p<0.05, ** p<0.01 and *** p<0.001.

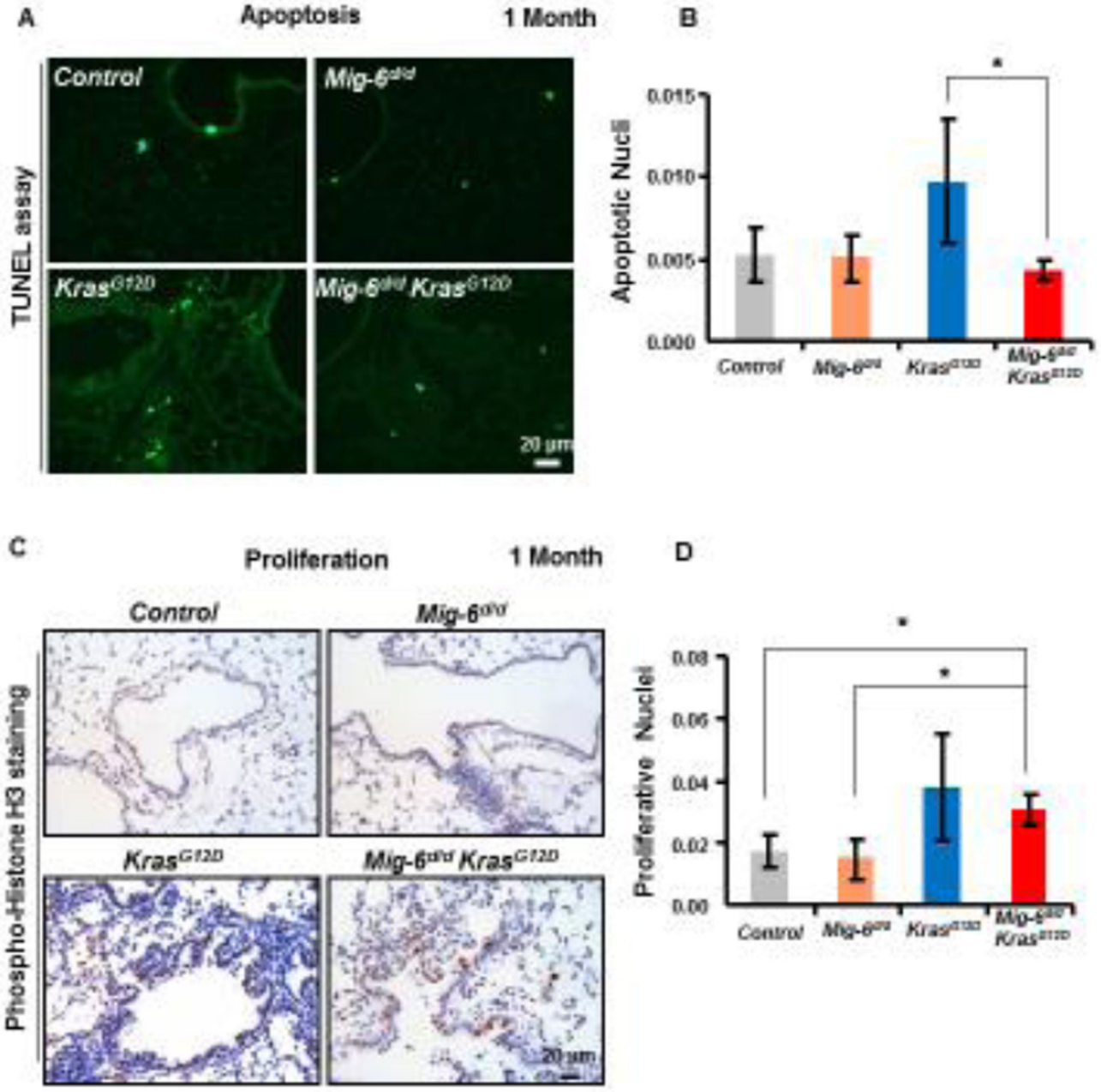

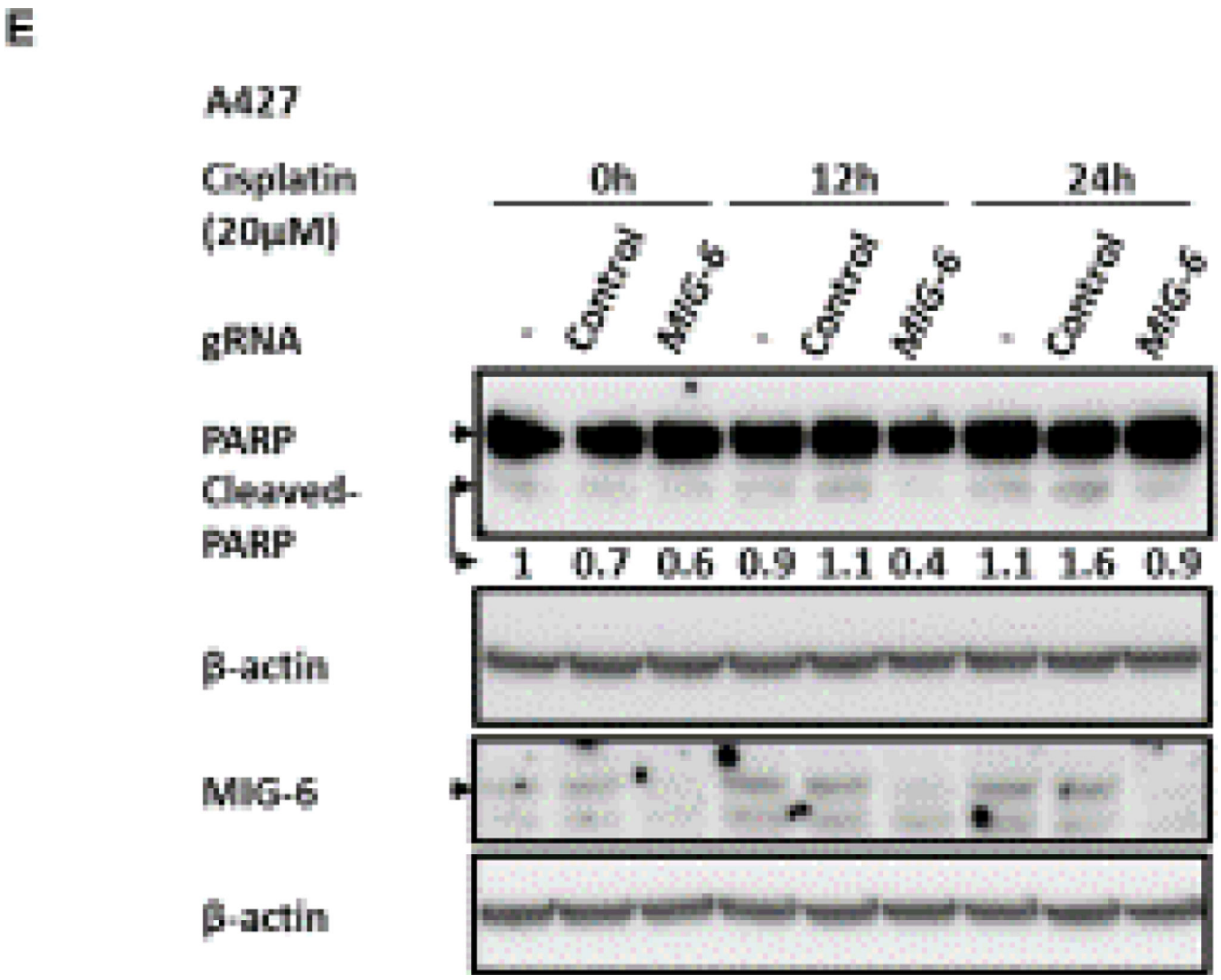

Figure 5. Ablation of *Mig-6* Reduced Apoptosis in *Kras*^{G12D}-driven Tumors

(A) TUNEL assay in the lungs of control, *Mig-6*$^{d/d}$, *Kras*^{G12D}, and *Mig-6*$^{d/d}$*Kras*^{G12D} mice (1 month of age). Apoptotic cells stained bright green. (B) Quantification of apoptotic cells in the lungs of control, *Mig-6*$^{d/d}$, *Kras*^{G12D}, and *Mig-6*$^{d/d}$*Kras*^{G12D} mice. *p<0.05. (C) Phospho-Histone H3 staining in the lungs of control, *Mig-6*$^{d/d}$, *Kras*^{G12D}, and *Mig-6*$^{d/d}$*Kras*^{G12D} mice (1 month of age). (D) Quantification of proliferative cells (phospho-histone H3 positive) cells in the lungs of control, *Mig-6*$^{d/d}$, *Kras*^{G12D}, and *Mig-6*$^{d/d}$*Kras*^{G12D} mice. *p<0.05. At least 4 left lungs of control, *Mig-6*$^{d/d}$, Kras^{G12D}, and *Mig-6*$^{d/d}$*Kras*^{G12D} mice were used in the quantification and at least 10 random areas from each lung were measured. Fluorescein positive nuclei or phospho-Histone H3 positive nuclei were counted and the percentages of positively stained nuclei to total nuclei were calculated. (E) Western Blot (WB) analysis of apoptosis of A427 cells after knock-out of *MIG-6* with or without treatment of Cisplatin. Cleaved-PARP is a typical indicator of apoptosis.

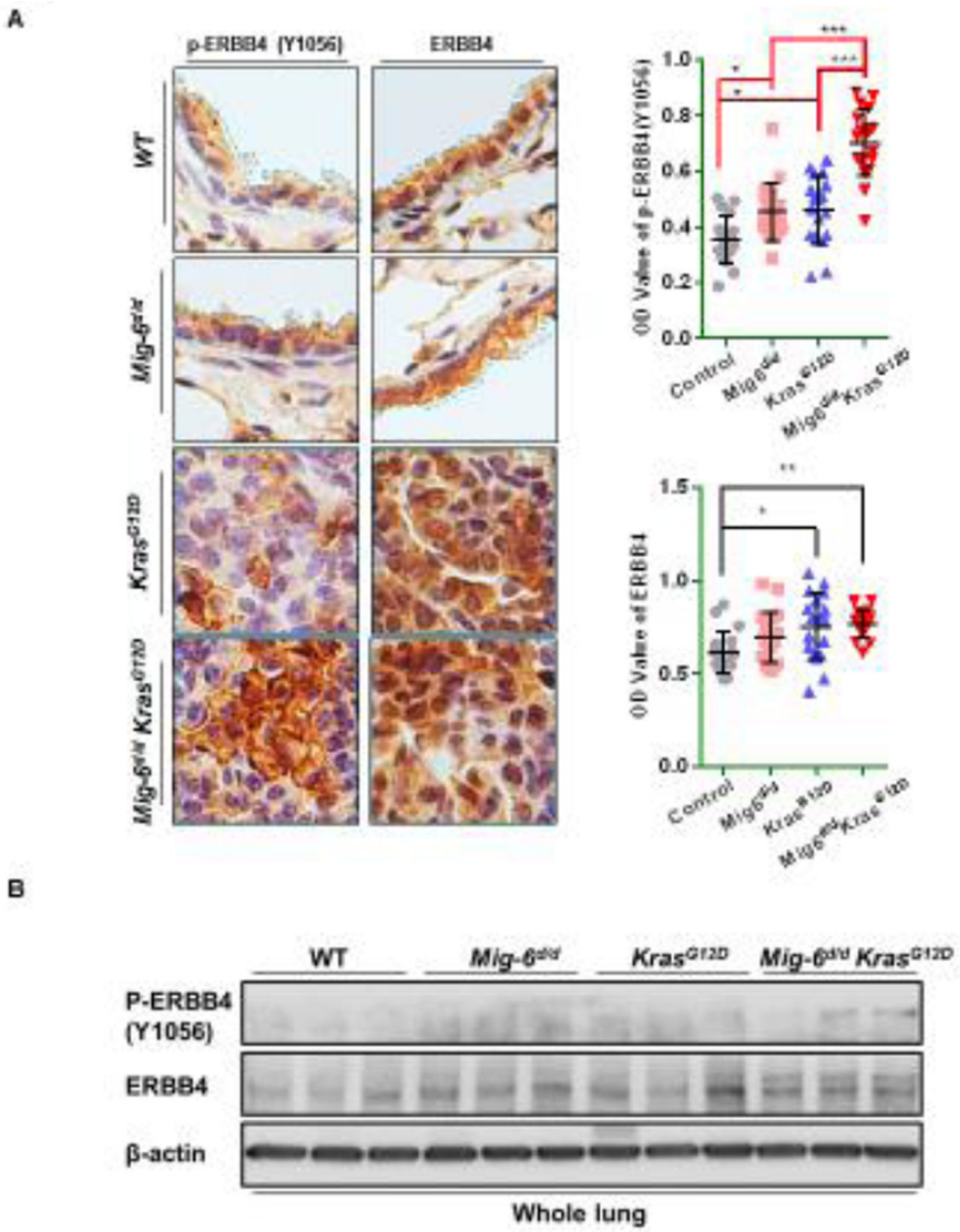

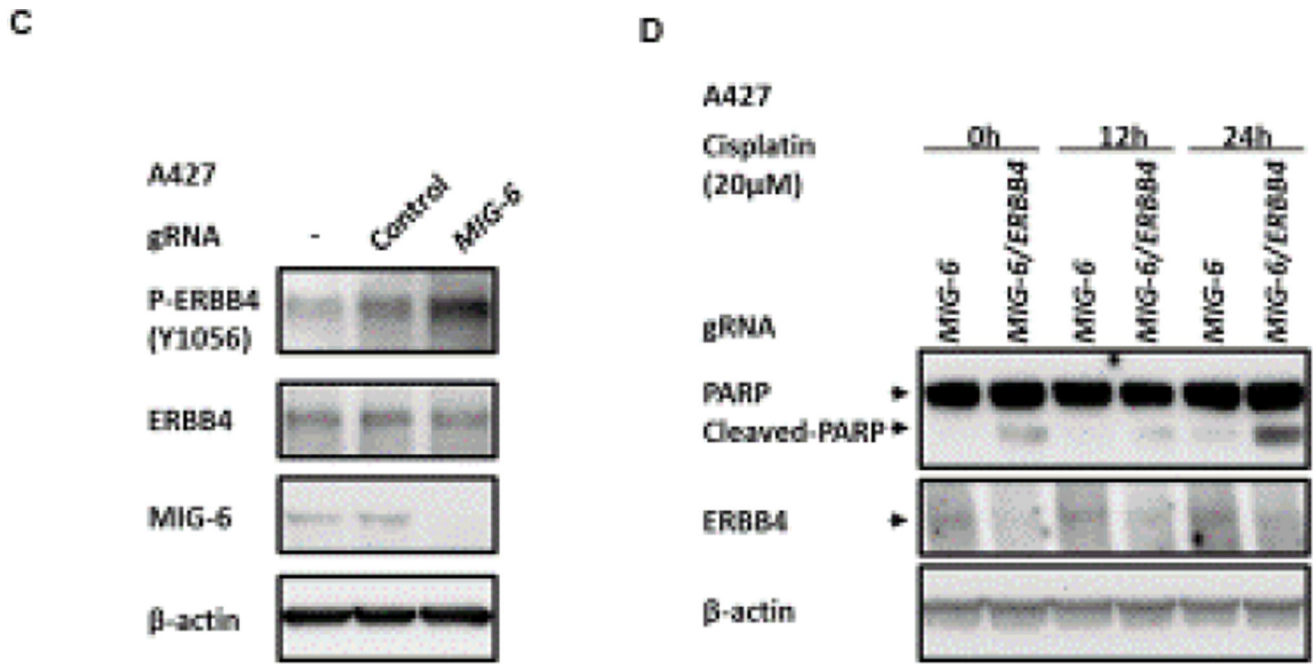

Figure 6. ErbB4 pathway was activated in lung tumor (*Mig-6*$^{-/-}$*Kras*^{G12D}) and attenuated apoptosis

(A and B) Immunohistochemistry (A) and WB (B) analyses of total and phosphorylated (p-) ERBB4 proteins in lung and lung tumors of 2-month old mice. (A) Left panel: IHC staining results are the representative results for each group; Right panel: quantification results are calculated from three mice per group (six regions for each mouse) using Image J [60]. Optical Density (OD) = log (max intensity/Mean intensity). The blue dashes point the area for the quantification. (B) WB analyses of total and p-ERBB4 proteins in lung of 2-month old mice. (C) WB analysis of p-ERBB4 in A427 cells after knock-out of *MIG-6*. (D) WB analysis of apoptosis of A427 cells after knock-out of *MIG-6* or *MIG-6/ErbB4* with or without treatment of Cisplatin.